Interferometric direct imaging properties of a BIGRE-DAM device in laboratory

Fabien Patru[a], Jacopo Antichi[a], Patrick Rabou[b], Enrico Giro[c], Jacopo Farinato[c], Raffaele Gratton[c], Daniele Vassallo[c], Christophe Verinaud[b], Denis Mourard[d], Julien Girard[e]

[a] Osservatorio Astrofisico di Arcetri, Firenze, Italia
[b] Institut de Planétologie et d'Astrophysique de Grenoble, Grenoble, France
[c] Osservatorio Astronomico di Padova, Padova, Italia
[d] Observatoire de la Cote d'Azur, Nice, France
[e] European Southern Observatory, Vitacura, Chile

ABSTRACT

DAM (Discretized Aperture Mapping) is an original optical concept able to improve the performance in high angular resolution and high contrast imaging by the present class of large telescopes equipped with adaptive optics. By discretizing the entrance pupil of a large telescope into an array of many coherent sub-apertures, DAM provides unique imaging and filtering properties by means of spatial filtering and interferometric techniques. DAM can be achieved by means of single-mode fibers, integrated optic waveguides, pinholes, or simply with an innovative BIGRE optical device. BIGRE is formed of an afocal double micro-lenses array. In addition to the pupil discretization process by spatial filtering, BIGRE can also provide two other optical processes: the pupil densification or the pupil dilution. DAD (Discretized Aperture Densification) increase the sub-aperture sizes and is suitable to a hypertelescope, whereas DADI (Discretized Aperture Dilution Interferometry) reduces the sub-aperture sizes and turns a large telescope into a Fizeau interferometer. This paper deals with the first in-lab experiment at visible wavelength of BIGRE devices for the three configurations above. We study the point spread function (PSF) when observing a point-like object located either on-axis or at various off-axis positions across the field of view. Both interferometric and diffractive effects are described. The experimental measurements are in good agreement with the BIGRE theory. It results that BIGRE fulfils the requirements to carry out spatially filtered pupil discretization (DAM), with possible densification (DAD) or dilution (DADI).

Keywords: pupil discretization, pupil densification, pupil dilution, interferometry, spatial filtering, double micro-lenses array, spatial aliasing, laboratory prototype

1. INTRODUCTION

DAM (Discretized Aperture Mapping) is an original optical concept able to improve the performance in high angular resolution and high contrast imaging by the present class of large telescopes equipped with adaptive optics (1; 2; 3). By discretizing the entrance pupil of a large telescope into an array of many coherent sub-apertures, DAM provides unique imaging and filtering properties by means of spatial filtering and interferometric techniques. DAM can be achieved by means of single-mode fibers, integrated optic waveguides, pinholes, or simply with an innovative BIGRE optical device. BIGRE is formed of an afocal double micro-lenses array (4; 5). In addition to the pupil discretization process by spatial filtering, BIGRE can also provide two other optical processes: the pupil densification or the pupil dilution. DAD (Discretized Aperture Densification) increase the sub-aperture sizes and is suitable to a hypertelescope, whereas DADI (Discretized Aperture Dilution Interferometry) reduces the sub-aperture sizes and turns a large telescope into a Fizeau interferometer.

Further author information: (Send correspondence to Fabien Patru and Jacopo Antichi)
Fabien Patru: E-mail: fabienpatru@gmail.com
Jacopo Antichi: E-mail: antichj@gmail.com

Optical and Infrared Interferometry and Imaging V, edited by Fabien Malbet, Michelle J. Creech-Eakman, Peter G. Tuthill, Proc. of SPIE Vol. 9907, 99072U
 · doi: 10.1117/12.2233108

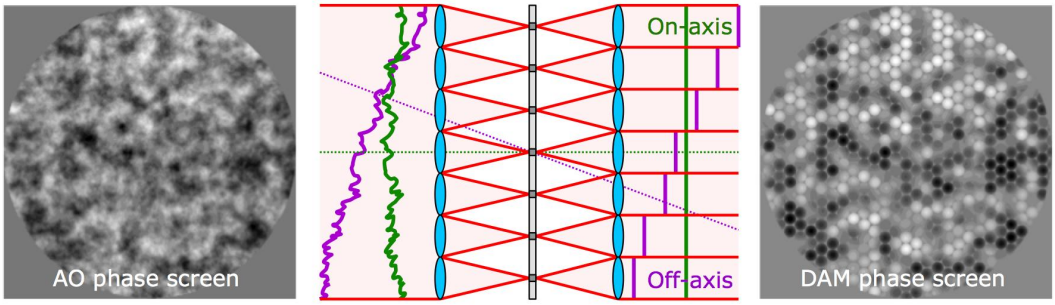

Figure 1. DAM optical scheme: The DAM device is composed of a double lenslet array matched with a filter array. Each sub-beam is diaphragmed by a lenslet, focussed into a spatial filter, and re-expanded onto a co-axial lenslet. DAM thus transforms a continuous and aberrated wavefront (on the left) into a discretized and smoothed wavefront (on the right). The small scale aberrations are spatially filtered within each sub-aperture (high spatial frequency rejection). An on-axis object (green line) transmits a flat wavefront while an off-axis object (violet line) yields a stair-shaped wavefront, thus preserving the tip-tilt information (low spatial frequency transmission). An off-axis object beyond the field of view imposed by the filter size is not transmitted.

We describe those new concepts of DAM, DAD and DADI relying on different technological solutions (Sect. 2). We show how BIGRE is an alluring solution to carry out spatially filtered pupil discretization, as well as pupil densification or dilution (Sect. 3). This paper deals with the first in-lab experiment at visible wavelength of BIGRE devices for the three configurations above (Sect. 4). In particular, we study the point spread function (PSF) when observing a point-like object located either on-axis or at various off-axis positions across the field of view. Both interferometric and diffractive effects are shown. The experimental results are in good agreement with the BIGRE theory. The next objectives are discussed to improve those preliminary results (Sect. 5).

2. OPTICAL CONCEPTS OF PUPIL DISCRETIZATION

2.1 Discretized Aperture Mapping (DAM)

Discretized Aperture Mapping (DAM) is a novel optical process of *pupil discretization*, where a continuous aperture is splitted into a finite number of discrete sub-apertures. As stated in mathematics, the *discretization* refers to the process of dividing a continuous object into a finite number of discrete elements. DAM is achieved by means of a compact optical device, combining both techniques of interferometry and spatial filtering. The concept and the formalism of the *pupil discretization* (1; 2; 3) has some analogy with the one of the *pupil segmentation* (6; 7), the *pupil remapping* (8) and the *pupil densification* (9; 10; 11; 12) possibly using single-mode fibers (13; 14).

DAM is placed through a collimated beam in a pupil plane conjugated with the entrance aperture. The DAM device is composed of a double lenslet array (namely two micro-lens arrays) matched with a spatial filter array located in the intermediate focal plane (Fig. 1). Each sub-beam is diaphragmed by a lenslet, focussed into a spatial filter to become coherent in phase, and re-expanded onto a co-axial lenslet to provide a collimated filtered sub-beam. The whole aperture is encoded into a mosaic of discrete sub-apertures. DAM thus transforms a continuous and aberrated wavefront into a discretized and smoothed wavefront. While the coherent sub-apertures become flat in phase, the differential pistons (namely the differential phases at a given wavelength) is passed between each pair of sub-apertures. The incoming wavefront is encoded into a set of photometric and pistonic - plus eventually tip-tilt - values.

This new filtering device provides unique filtering and imaging properties to clean-up either a wavefront or an image. DAM optically smooths an aberrated wavefront in a pupil plane and improve the perceptible contrast in an image plane by removing scattered light (Fig. 2). DAM seems therefore suitable for both wavefront sensing (3) and direct imaging applications (2). First, it enables passive wavefront filtering of high-order aberrations. DAM can be used as a high spatial frequency filter to remove out the small scale defects in any optical system limited by high-order aberrations. Second, it allows high angular resolution and high contrast imaging, by restoring

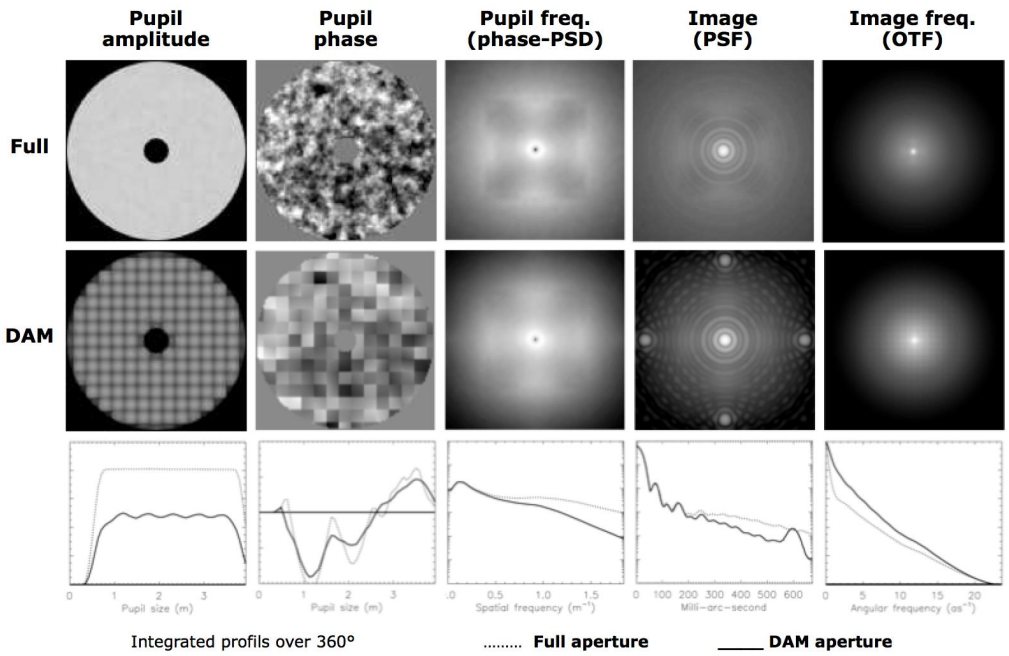

Figure 2. DAM optical properties (from left to right): aberrated wavefront in the pupil shown in amplitude and in phase, pupil spatial frequency content shown by the phase power spectral density (phase-PSD), aberrated image or point spread function (PSF), image angular frequency content shown by the optical transfer function (OTF). Comparison between solely the full aperture (top, dashed line) and the DAM aperture using a filter (bottom, solid line). DAM smooths the amplitude and phase aberrations in the pupil by attenuating the high spatial frequencies in the phase-PSD. Conversely, DAM dims the scattered halo and improves the contrast in the image by attenuating the low angular frequency aberrations in the OTF and by enhancing the high angular information. Consequently, the residual aberrations which cannot be corrected by an adaptive optics system are purely and simply removed by discretizing the wavefront by means of a DAM device.

diffraction limit and high dynamic range on a finite field of view. DAM remains invariant by translation in the focal plane when pointing an off-axis object, preserving the object-image convolution relationship and rendering possible deeper contrasted images at high angular resolution.

DAM provides in the focal plane an "in-between" PSF, combining both interferometric and diffractive properties. The fringes appears within an Airy envelope, due to the discretization of a single aperture into many sub-apertures. The theoretical PSF can be written as the product of a diffraction pattern and an interference pattern. The diffraction pattern is the sum of the Airy functions delivered by each coherent sub-aperture. The interference pattern is the sum of the fringe cosine functions produced by each pair of sub-apertures.

2.2 Discretized Aperture Densification (DAD)

It has been shown that a hypertelescope (9; 10; 11) can provide snapshot images with a long baseline interferometer and a densified pupil combiner. By increasing the relative size of the beams and by preserving the baseline arrangement, a pupil densifier transforms a diluted aperture into a dense aperture suitable for direct imaging. A multi-axial recombination in the focal plane concentrates all the flux in the real usable field of view, yielding a significant gain in sensitivity compared to the Fizeau mode. The flux is focused within a window function matching the useful field of view, minimizing the interferometric side-lobes and maximizing the encircled energy in the central lobe, without any loss of angular resolution information contained in the interference pattern.

In addition, using a densified pupil combiner based on single-mode fibers improves the high contrast imaging performance (10; 13; 14), by combining two optical processes that are the densification and the discretization. Spatial filtering greatly enhances the quality and the stability of the densified image, but partially decreases the flux throughput (13). Moreover, the use of single-mode fibers may simplify the image deconvolution process (1) and the beams cophasing technique (15).

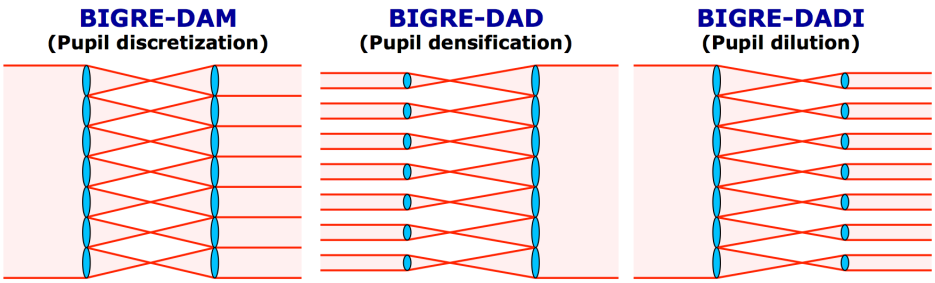

Figure 3. Optical schemes for DAM, DAD and DADI. Each lenslet is formed by two micro-lenses having the same diameter but a different focal length, providing, respectively, pupil discretization, pupil densification and pupil dilution.

DAD (Discretized Aperture Densification) transforms a diluted entrance pupil into a densified and discretized exit pupil, suited to long baseline interferometry for direct imaging applications. DAD yields the same spatial filtering and imaging properties than DAM with, in addition, an optical densification process. A pupil densifier based on micro-lenses arrays should be explored as an easy and robust solution. Such light and compact DAD device could be easily mounted on the gondola of a hypertelescope, like the projects Carlina (16) or Ubaye (17).

2.3 Discretized Aperture Dilution Interferometry (DADI)

We would like to introduce further an original concept of *pupil dilution*. The pupil dilution consists in decreasing the relative size of the sub-apertures, contrary to the pupil densification which increase it. Thus, the idea is no more to densify the pupil of a large array of telescopes, but to dilute the pupil of a single telescope. The entrance aperture is transformed into many small sub-apertures with large gaps in between, as for a Fizeau interferometer.

DADI (Discretized Aperture Dilution) transforms a full entrance pupil into a diluted exit pupil, suited to Fourier imaging applications with large telescopes. DADI yields the same spatial filtering and imaging properties than DAM with, in addition, an optical dilution process. Fourier imaging can be achieved on a single aperture by modifying the entrance pupil, either by choosing a non-redundant arrangement of the baselines with a mask made of holes (SAM (18)), or by rearranging the baselines to avoid redundancy by means of a bundle of single-mode fibers (FIRST (8)), or newly by reducing the size of the beams while preserving the arrangement of the baselines with a compact device (DADI).

DADI, in its basic configuration, produces however a redundant Fizeau interferometer. Considering redundant *vs* non-redundant baselines in the array distribution, the techniques usually rely on a non-redundant array for Fourier imaging applications (SAM (18), FIRST (8)), but the new Kernel-phase approach (19) proposes to use a redundant array, assuming a high Strehl regime. Indeed, for a poor Strehl regime, the Fourier components - (u, v) samples - are mixed due to differential pistons between redundant baselines. The only way to disentangle the signal is to use a non-redundant array. In contrast, in a high Strehl regime, the Fourier components add - almost - coherently, by preventing differential pistons. This approch preserves and amplifies the signal by adding the same measurement probed several times by few redundant baselines. Consequently, DADI could be applied to Fourier imaging with an AO-equipped telescope providing a high Strehl regime.

2.4 Comparison between the concepts

The pupil discretization (DAM), the pupil densification (DAD) and the pupil dilution (DADI) all rely on a discretized aperture where each sub-aperture is spatially filtered to remove high spatial frequency aberrations while the distribution of the sub-apertures centers is maintained to provide directly an image in the focal plane (10) (Fig. 3). The pupil discretization (DAM) preserves the shape and size of each sub-aperture from the entrance to the output, providing spatial filtering properties only. In addition to the discretization, the pupil dilution (DADI) reduces the relative size of the beams to turn a direct imager into an interferometer, whereas the pupil densification (DAD), inversely, increase the relative size to turn an interferometer into a direct imager. While DAM and DAD are dedicated to direct imaging, DADI could allow Fourier imaging.

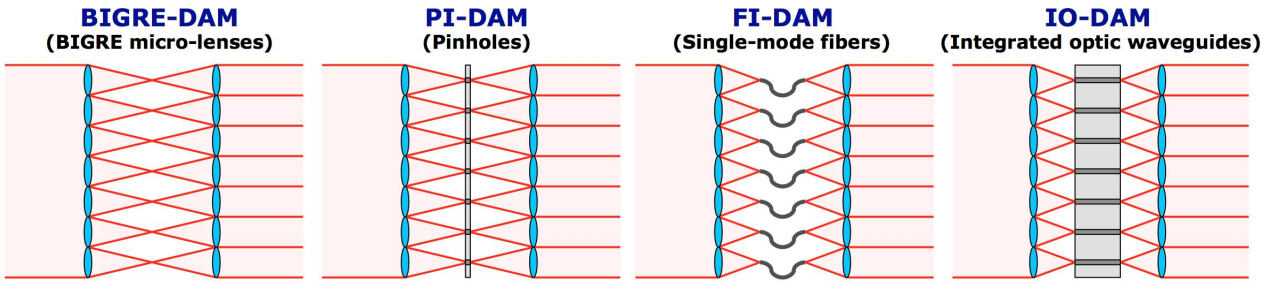

Figure 4. DAM technological solutions: The double lenslet array is matched with a spatial or modal filter array, providing respectively multi-mode or single-mode filtering properties. DAM can rely on spatial filtering by using an array of pinholes (PI-DAM) or solely a fine-tuned double lenslet array (BIGRE-DAM). DAM can rely on modal filtering by using an array of waveguides, either with a three-dimensional integrated optic composed of photonic circuits (IO-DAM) or with a bunch of single-mode fibers (FI-DAM).

DAM concept	BIGRE-DAM	PI-DAM	IO-DAM	FI-DAM
Sub-apertures device	Micro-lenses	Micro-lenses	Micro-lenses	Micro-lenses
Filter device	2nd lens	Pinhole	Int.opt.waveguide	Single-mode fiber
Spatial/Modal filtering	Spatial filtering	Spatial filtering	Modal filtering	Modal filtering
Number of sub-apertures	High	High	Moderate	Low
Field of view	Moderate	Moderate	Moderate	Small
Flux throughput	Moderate	Moderate	Moderate	Moderate
Complexity	Low	Moderate	Moderate	High
Need of R&T	Low	Low	High	Moderate

Figure 5. DAM technological solutions: Those solutions have their own pros and cons, and varying levels of complexity and development, so that the technological choice will be driven by the scientific requirements.

2.5 Comparison between the technological solutions

DAM, DAD, and DADI can be achieved with different technological solutions. The phase defects can be removed in each sub-pupil either by spatial filtering or by modal filtering, providing respectively multi-mode or single-mode filtering properties (20). Both techniques improves the spatial coherence of the filtered wavefront, by transmitting most of the coherent light (in the Airy disc) and rejecting most of the incoherent light (in regions outside the Airy disc). While modal filtering transmits a single fundamental mode which is free of phase defects, spatial filtering is still multi-mode and lets pass through part of the incoherent light. Modal filtering is thus more efficient but more complex and expensive than spatial filtering. We propose alternative technological solutions based on single-mode or multi-mode spatial filtering (Fig. 4). Those solutions have their own pros and cons, and varying levels of complexity and development (Fig. 5), so that the technological choice will be driven by the scientific requirements.

3. BIGRE OPTICAL DEVICES FOR PUPIL DISCRETIZATION

3.1 The BIGRE optical device

DAM, DAD, and DADI can be achieved with a BIGRE double lenslet array (4) - made of micro-lenses - mounted in a pupil plane conjugated with the entrance aperture of the telescope. Initially used for integral field spectroscopy (4), BIGRE has been turned into a spatial filter and re-imager to perform the pupil discretization (5). BIGRE is a light, compact and robust device, easy to integrate and to operate. The optical device is rather cheap (few ten k€), even with a large number of sub-apertures (few tens to thousands). It is the simplest and the cheapest option among the technological solutions above.

BIGRE is composed of two consecutive micro-lenses array set in an afocal configuration. Each couple of input-output micro-lenses induces a spatial filtering in the intermediate focal plane conjugated with the detector plane. By adjusting the focal lengths of the two micro-lenses, the irradiance of each beam is diaphragmed by the exit surface of the second micro-lens enough to transmit only the central Airy peaks (5). Thus, the last

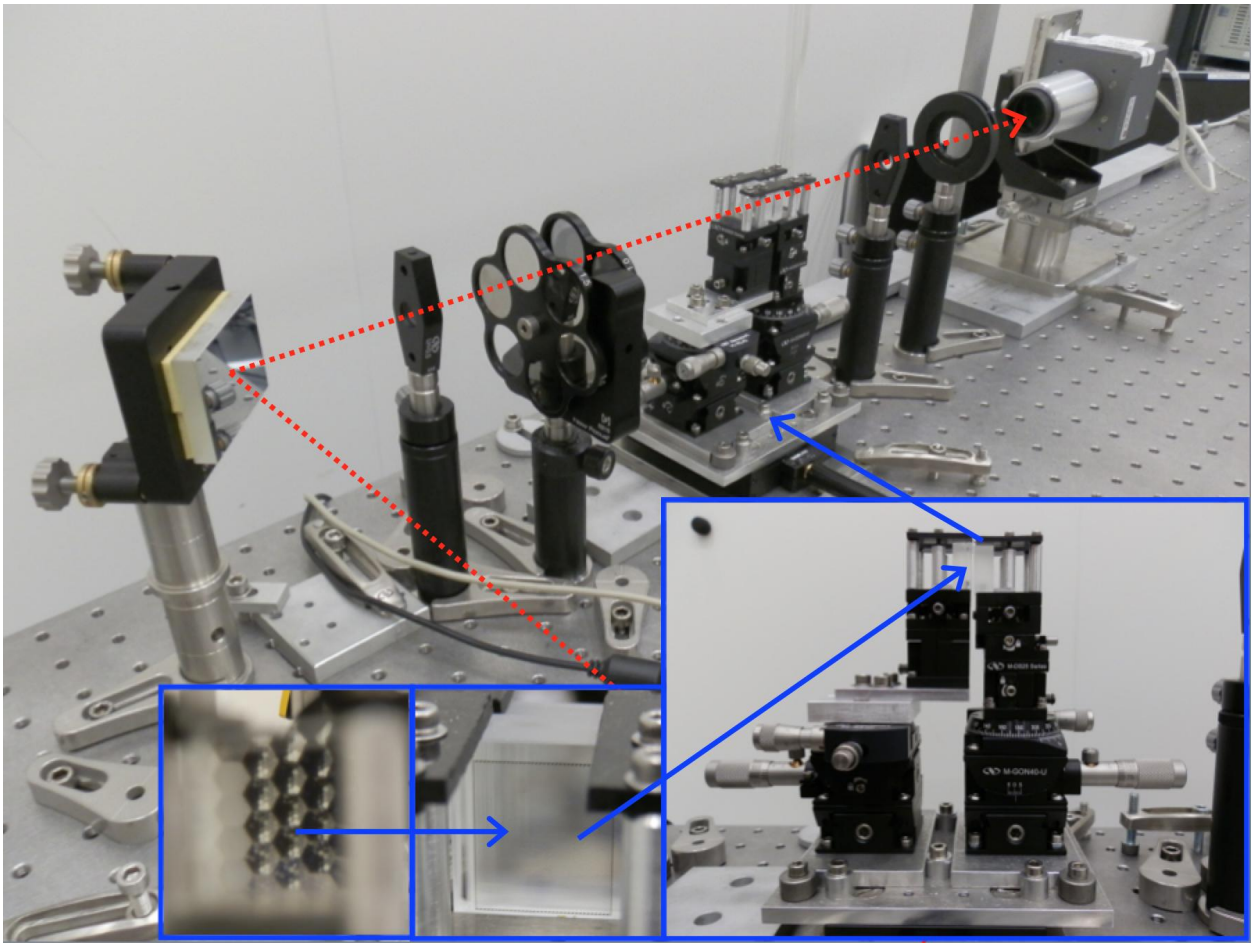

Figure 6. VISIDAM testbed to characterize the BIGRE devices. The entrance beam reflects on a mirror, is collimated by a lens, passes through a density, propagates through the BIGRE device and is finally focalized by a lens onto a CCD camera (from left to right, following the red arrow). Some details of the BIGRE device are shown (blue boxes).

micro-lens re-images a spatially filtered sub-aperture having a Gaussian profile, while the whole recombined sub-images produces a focal image having interferometric and diffractive properties. Finally, BIGRE provides an equivalent spatial filtering in the intermediate focale plane between the two lenslet arrays in order to reject the - unwished - cross-talk light outside of the CCD camera, while the scientific light is focused on it.

3.2 Dimensioning

By carefully designing the geometry of a double micro-lenses array, one can finely tune a BIGRE as a function of the scientific application. The BIGRE devices offer flexibility to adjust internal parameters for designing various setups. The main parameters that can be optimized are as follows:

- The working wavelength λ. We consider here the visible wavelength at $\lambda = 0.633\mu m$. BIGRE can be designed as achromatic on a narrow bandwidth (5).
- The lenslet pitch s, or the linear number of sub-apertures N across the pupil diameter. The lenslet pitch is chosen to adjust the interferometric field of view of BIGRE with the field of view required of the experiment.
- The array geometry, defined by the shape, the size and the distribution of the sub-apertures (square, hexagonal, circular shape).
- The spatial filtering level N_{Airy}, defined as the number of Airy rings transmitted by the spatial filter. In practice, $N_{Airy} = 2.5$ is optimum to transmit only the Airy disc and to mitigate the chromatic effects (4).

- The magnification factor m between the input and output sub-aperture sizes: $m = d_o/d_i$. The magnification factor offers different modes of observation, as follows:
  - DAM (1:1 magnification with $m = 1$) for direct imaging with a single aperture telescope,
  - DAD (densification with $m > 1$) for direct imaging with a long-baseline interferometer,
  - DADI (dilution with $m < 1$) for Fourier imaging with a telescope.

3.3 Strategy for the experiment

In this experiment, we have used two identical BIGRE devices, which have been initially designed as prototypes for SPHERE-IFS. Natural K factor (4) of these BIGRE spares is 5.45 when adopted in a focalized beam in IFS usage. Each lenslet array has the same pitch $P = 200\mu m$ but a different focal length (the ratio F_1/F_2 equals to $K = 5.45$). The thickness of the two lenslet arrays equals to $T = 7.53mm$. The material (Suprasil 3001) provides an index of refraction $n = 1.46$ at $633nm$, as fixed in this experiment by the laser source ($\lambda = 0.633\mu m$). The broad-band transmission of the material in use (Suprasil 3001) covers the range $0.18 - 3.50\mu m$. The devices have been designed in the visible wavelengths ($0.55 - 0.65\mu m$ in R band). It is made of an hexagonal array of circular or hexagonal sub-apertures. Only one surface - corresponding to the first surface for BIGRE-IFS - is masked circularly onto each hexagonal micro-lens with a black chromium deposit at 95% of the pitch ($mask = 0.95$).

Those BIGRE devices have been characterized on the VISIDAM testbed (Fig. 6) at the Observatoire de la Côte d'Azur (OCA), in such a way to reproduce a discretized aperture scheme. According to the DAM concept, the BIGRE is now placed in a collimated beam having a diameter equal to $D = 10mm$. The beam is focused downstream onto a CCD detector to image the PSF. BIGRE can be oriented in the same direction of propagation as for SPHERE-IFS (namely BIGRE[+1]) or in the inverse direction of propagation (namely BIGRE[−1]). In this paper, we have exploited three different configurations, as follows:

- BIGRE[+1] *a priori* equivalent to DADI for pupil discretization and dilution,
- BIGRE[−1] *a priori* equivalent to DAD for pupil discretization and densification,
- BIGRE[+1−1], combining BIGRE[+1] & BIGRE[−1], *a priori* equivalent to DAM for pupil discretization.

4. BIGRE OPTICAL DEVICES AT WORK IN LABORATORY

4.1 Spatial filtering through each sub-apertures

According to the basic equation of BIGRE (5): $N = (P^2 \cdot mask)/(T \cdot \lambda) \cdot n$, the spatial filtering level reaches $N = 11.61 \approx 12$. This equation is independent on the [+1], [−1] signatures. The system has been defined as to project on the second surface $11.61 \approx 12$ Airy rings. The number of interferometric side-lobes inside the first minima of the Window function is 12, just because the number of Airy rings projected onto the second BIGRE surface is 12. The number of side-lobes inside the first minima of the Airy pattern in the BIGRE[+1] mode is the same as in the case of BIGRE[−1]. This is due to the fact that the projection of the Airy pattern made by the first micro-lens onto the second micro-lens of the BIGRE is the same, whatever the orientation it gets. Spatial filtering by a BIGRE lenslet array is verified only in the [−1] mode, while in the [+1] mode there is a perfect stigmatic imaging of the global Airy pattern diffracted by each single BIGRE first micro-lens.

4.2 Interferometric and diffractive features of the PSF

The camera lens projects the internal Airy pattern in the final focal plane in a way which is common to each sub-aperture (what we called meta-pupil in the IFS mode). The far-field (Fig. 7) is quasi-equivalent to an extra-focal image (Fig. 8) and is directly related to the focal pattern (Fig. 8) re-imaged by the camera lens. Whatever the BIGRE configuration ([+1], [−1] or [+1−1]), the point spread function (PSF) has common features:

- a central Airy pattern within the useful field of view of width λ/P (not resolved here due to low resolution),
- a central diffraction lobe - an Airy disc - with its inner working angle large as λ/D,
- an interference pattern made of interferometric side-lobes regularly spaced with a mutual distance equal to λ/P and distributed onto an hexagonal pattern (induced by the hexagonal array of sub-apertures),
- a Window function of width $N\lambda/P$ (produced by each individual sub-aperture being - or not - filtered).

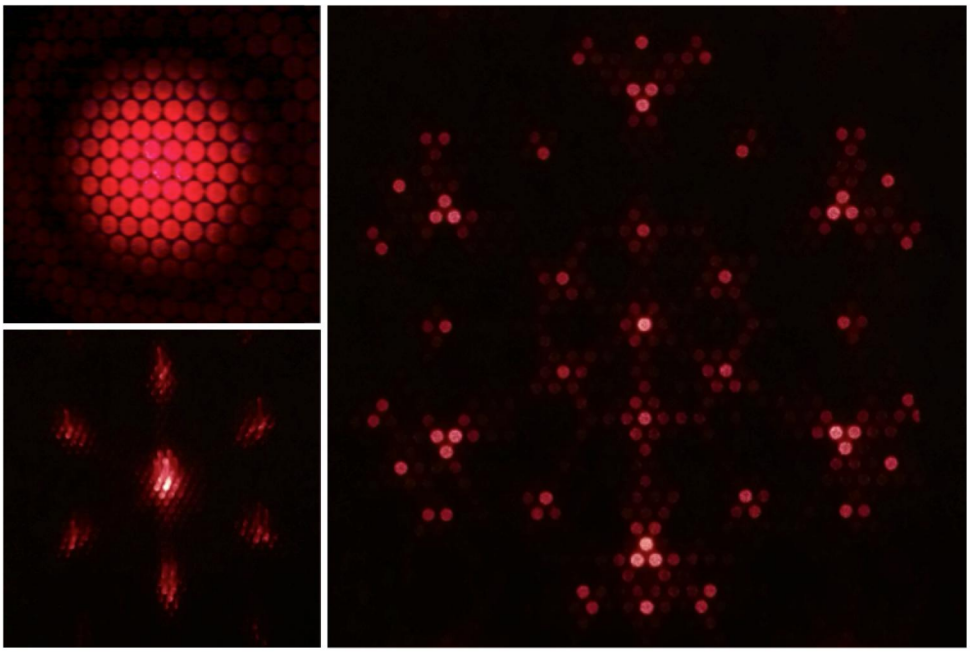

Figure 7. Far-field projected onto a wall by removing the focalization lens and the camera for BIGRE[+1] (top left), BIGRE[−1] (right) and BIGRE[+1−1] (bottom left). For BIGRE[+1−1], the coherent light remains concentrated on-axis while the scattered light is rejected in six surrounding areas, due to the hexagonal distribution of the lenslets.

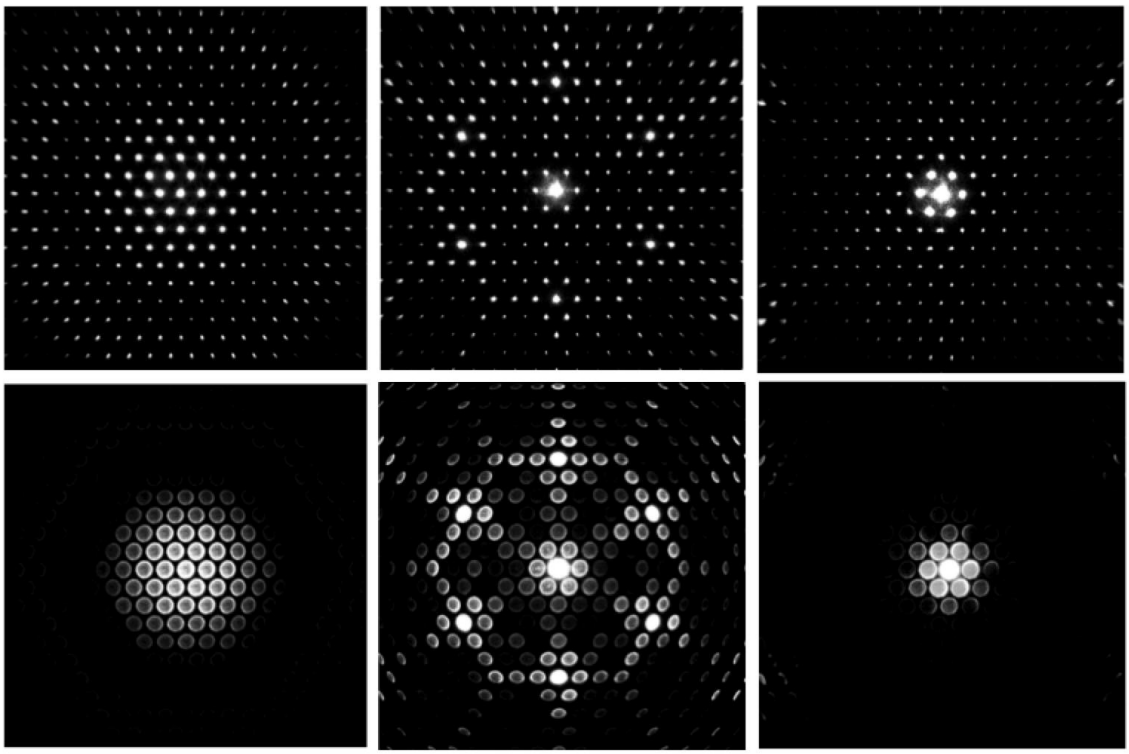

Figure 8. Focal plan (top) and extra-focal plan (bottom) for BIGRE[+1] (left), BIGRE[−1] (middle) and BIGRE[+1−1] (right).

Thus, the final image is an interferometric PSF made by the product of two terms: a Comb function times a Window function. The Comb function is made of interferometric side-lobes which are regularly spaced. The Window function can be approximated by a somewhat Gaussian shape, as expected by the BIGRE theory on the slit function (4)). The Window function in the densified or discretized image of BIGRE[−1] or BIGRE[+1−1] is narrower than the Window function obtained in the Fizeau image of BIGRE[+1].

4.3 BIGRE[+1]

BIGRE[+1] is a single BIGRE oriented in the same direction as the SPHERE IFS configuration, but through a collimated beam. The input focal length is larger than the output focal length ($F_1 > F_2$). We are in the case of a dense pupil remapped into a diluted pupil, *i.e.* a full aperture turned into a finite number of small sub-apertures. The sub-aperture width - the beam diameter - is reduced by a factor $m = F_2/F_1 = 1/5.45$. The magnification factor - below 1 - is called the dilution factor. The dilution factor $m = 1/5.45$ is the inverse of the demagnification factor $K = F_1/F_2 = 1/m$ defined for BIGRE used in SPHERE-IFS (4). BIGRE[+1] produces pupil dilution ($m < 1$) without spatial filtering ($N = 12$). The focal pattern of BIGRE[+1] is a perfect Fizeau image (Fig. 8), *i.e.* a Comb function multiplied by a large Window function. The Window function approaches an Airy pattern.

In the BIGRE[+1] mode, there is no spatial filtering at the second BIGRE surface. The light that exceeds the second surface (*i.e.* from 12 Airy rings up to infinity) and going onto the neighbouring lenses is imaged outside the BIGRE in a convergent way, but the camera lens restores the correct propagation in a way allowing to consider the camera lens as a perfect Fourier transform of the internal Airy pattern formed inside each micro-lens. There are about 12 lobes within the Window function with distance to each other equal to λ/P, as expected and as it appears in the raw images (Fig. 8).

4.4 BIGRE[−1]

BIGRE[−1] is a single BIGRE oriented inversely to the SPHERE IFS configuration. The input focal length is smaller than the output focal length ($F_1 < F_2$). We are in the case of a dense pupil remapped into a hybrid pupil, *i.e.* a full aperture turned into a discrete aperture modified differently in amplitude within the sub-apertures. The sub-aperture width remains unchanged without magnification $m = 1$. BIGRE[−1] produces neither densification nor dilution ($m = 1$) and very low spatial filtering ($N = 12$). The focal pattern of BIGRE[−1] is a somewhat densified image (Fig. 8), *i.e.* a Comb function multiplied by a narrow Window function. The Window function is an unperfect Gaussian.

In the BIGRE[−1] mode, there is spatial filtering in the pupil plane at the second BIGRE surface. The light that exceeds the second surface (*i.e.* from 12 Airy rings up to infinity) and going onto the neighbouring lenses is imaged outside the BIGRE in a divergent way and is no more recovered by the camera lens. We can recognize, as expected, about 12 lobes within the Window function regularly spaced by λ/P (Fig. 8). The filtering onto the second BIGRE[−1] surface is not strong and so the global operation, *i.e.* the filtering and the Fourier transform made by the second lenslet surface, produces a Window function which is not-so-well Gaussian.

4.5 Holed mask BIGRE[−1]

BIGRE[−1] can be adopted in two ways: 1. without a holed mask at the front of it, providing a system with $m = 1$ and $N = 11.61$; 2. with a holed mask with holes diameters equal to P/m, providing a system with $m = 5.45$ and $N = 2.95$. Then, only a holed mask seems to be compliant to the spatial filtering requests of our experiments. We are in the case of a diluted pupil remapped into a densified pupil, *i.e.* a sparse aperture turned into large and contiguous sub-apertures. The sub-aperture width is increased by a factor $m = F_2/F_1 = 5.45$. The magnification factor $m = 5.45$ is thus equal to the densification factor γ defined for the hypertelescope ($m = \gamma$). Holed mask BIGRE[−1] produces densification ($m > 1$) and strong spatial filtering ($N = 3$). The focal pattern of Holed mask BIGRE[−1] is a real densified image, *i.e.* a Comb function multiplied by a narrow Window function. The Window function in this case is a quasi-Gaussian.

In this experiment, BIGRE[−1] has not been tested with a holed mask. For a well design setup, the manufacturer could deposit a black chromium mask onto the first surface of each micro-lens up to P/m. Otherwise, one can use a holed mask in front of BIGRE[−1] but it is not easy to manufacture it with tiny holes d and to

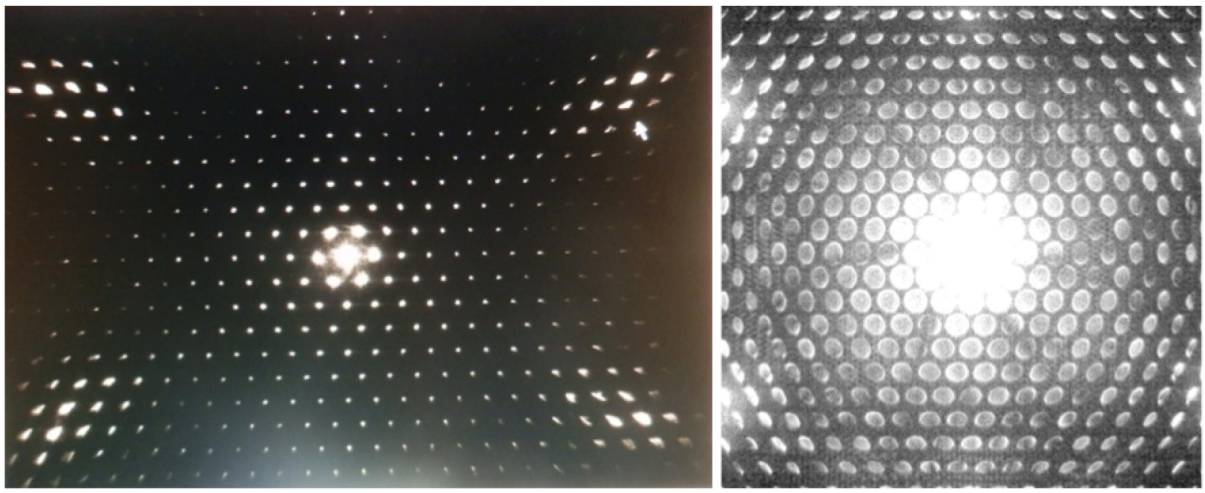

Figure 9. Focal plan across a wide-field (left) and extra-focal plan (right) with saturation for BIGRE[+1−1].

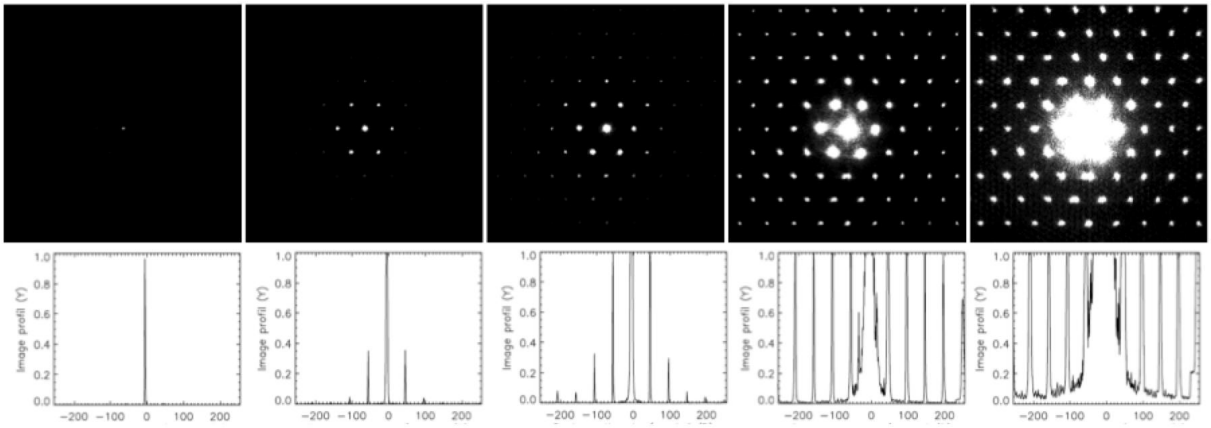

Figure 10. Focal plan for BIGRE[+1−1] with increasing level of saturation (by a factor 10, from left to right), highlighting the interferometric side-lobes within the Window function.

align it with BIGRE[−1]. Alternatively, the holed mask has been substituted by means of a BIGRE[+1] in front of BIGRE[−1], yielding the pupil discretization concept (Sect. 4.6). In fact, the holed mask is only useful for a laboratory test to properly validate the pupil densification scheme. In practice, for long baseline interferometry providing highly diluted apertures, the holed mask corresponds to the distinct beams coming from each telescope up to the pupil densification beam combiner. For applications onto a large telescope, the densification mode is useless due to a significant flux loss, while the pupil discretization makes sense (Sect. 4.6).

4.6 BIGRE[+1−1]

BIGRE[+1−1] is formed by two head-to-tail BIGRE[+1] and BIGRE[−1] devices aligned together. The magnification factor reduces to $m = 1$ with identical focal lengths $F_1 = F_2$. Thus, the system is afocal, yielding the same size of each entrance and exit sub-aperture. We are in the case of a dense pupil mapped into a discrete pupil, *i.e.* a full aperture turned into a finite number of spatially filtered sub-apertures. BIGRE[+1−1] produces pupil discretization ($m = 1$) - without densification or dilution - with a strong spatial filtering ($N = 3$). The focal pattern of BIGRE[+1−1] is a real densified image (Fig. 8, 9 & 10), *i.e.* a Comb function multiplied by a narrow Window function. The Window function is a real Gaussian function, thanks to a high level of spatial filtering onto each lenslet. Most of the flux is contained in the diffraction envelope windowing the central peak plus six neighbouring side-lobes, due to the hexagonal distribution of the lenslets.

The BIGRE[+1−1] setup is equivalent to holed mask BIGRE[−1] but provides $m = 1$ and strong spatial filtering $N \approx 3$. Instead of using a holed mask in front of BIGRE[−1], BIGRE[+1] effectively produces small entrance sub-pupils onto BIGRE[−1] with size P/m. This light is then spatially filtered by BIGRE[−1] according to the recipe: $m = 5.45$, $N = 2.95$. This allows a better spatial filtering that makes the Window function really Gaussian. But the fact that globally BIGRE[+1−1] is a $m = 1$ system, means that there is a rescaling so that the final Window function is really narrow with respect to the case BIGRE[+1].

Spatial filtering is well verified in this case of BIGRE[+1−1]. There is no cross-talk light that goes to the neighbouring lenses but coming out collimated or convergent. The pupil spatial filtering is not achieved in the intermediate focal plane but at the second lenslet surface. In the case of an afocal system providing $m = 1$, we can state that: "The pupil spatial frequencies at the second lenslet surface are only a rescaled version of the pupil spatial frequencies at the focal plane". According to Goodman (21) (see Introduction to Fourier Optics 4.2.4), between two coaxial spherical surfaces (first and second lenslets in this case), there is only a Fourier Transform without any Fresnel effect. So, the pattern at the second lenset surface is really the Fourier transform of the pattern at the first lenslet array.

4.7 Off-axis behaviour

We study next the off-axis behaviour of the light propagation through BIGRE for different off-axis position (Fig. 11 & 12). For BIGRE[+1], both the interference function and the Window function move on the same amount in the focal plane when pointing off-axis, thus providing a perfect convolution relationship, as expected in a Fizeau interferometer (10). On the opposite for BIGRE[−1] and BIGRE[+1−1], the diffraction envelope (or Window function) stays fixed on the center when pointing off-axis. Only the interference pattern - Comb function - is shifted. This result allows us to state that: "Spatial filtering cancels the tip-tilt induced by an off-axis source on the sub-aperture scale." This imaging property shows that BIGRE[+1−1] behaves the same as a modally filtered DAM design (*e.g.* based on single-mode fibers) (3; 10; 11).

The statement of Goodman (21) (given previously in Sect. 4.6) is very important in the case without magnification ($m = 1$), because we can take out all the issues related to misalignment between the diffraction envelope (Window function) and the interference pattern (Comb function), as it occur in the case of the pupil densification for a hypertelescope (5; 22). In fact, a hypertelescope only provides a pseudo-convolution relation: the envelope is slightly shifted off-axis, despite the approximation of fixed envelope with a highly diluted aperture. We assert that the pseudo-convolution relation of a hypertelescope (9) is strictly verified on a finite field of view (10) by means of a double BIGRE lenslet array set in a BIGRE[+1−1] configuration. The entire problem issued by various authors about the differential movement of the interference pattern *vs* the diffraction envelope is resolved. In fact, for BIGRE[+1−1], there is no more angular difference between the diffraction envelope and the interference pattern just for ray-tracing reasons. The envelope remains fixed off-axis. So, in this case we can say that a true object-image convolution relation holds within a small field of view. Speaking like such authors, for an off-axis point source, a double BIGRE lenslet array set as BIGRE[+1−1] produces a real stair-shaped profile, as expected, providing a fixed envelope inside which a true convolution is maintained.

4.8 Comparison between the BIGRE devices

BIGRE[+1] transforms a dense aperture into a diluted aperture producing a Fizeau image, but performs no spatial filtering. Although BIGRE[−1] is a hybrid device, a holed mask in front of BIGRE[−1] yields to a densification mode. Holed mask BIGRE[−1] transforms a diluted aperture into a densified aperture producing a densified image, but performs poor spatial filtering. The afocal device BIGRE[+1−1] transforms a full aperture into a discretized aperture producing a direct image, and performs efficient spatial filtering. To resume, we point up two fundamental properties for BIGRE[+1−1]:

1. It avoids the issue of a negative *vs* positive micro-lenses array by maintaining fixed the Window function.
2. It achieves a true filtering of the high spatial frequencies in a conjugated pupil plane.

From the point of view of the DAM *vs* BIGRE theory, DAM ($m = 1$) and DAD ($m > 1$) belong to same BIGRE concept. On the contrary, DADI ($m < 1$) exploits the BIGRE concept like in the SPHERE IFS case but on a pupil plane. Because in this case $F_1 > F_2$, there will be always diffracted light from elsewhere that may enter in the scientific beam of a single BIGRE unit as stray light. The unique way for producing spatial filtering would be using a pinholes mask in the intermediate focal plane (PI-DADI).

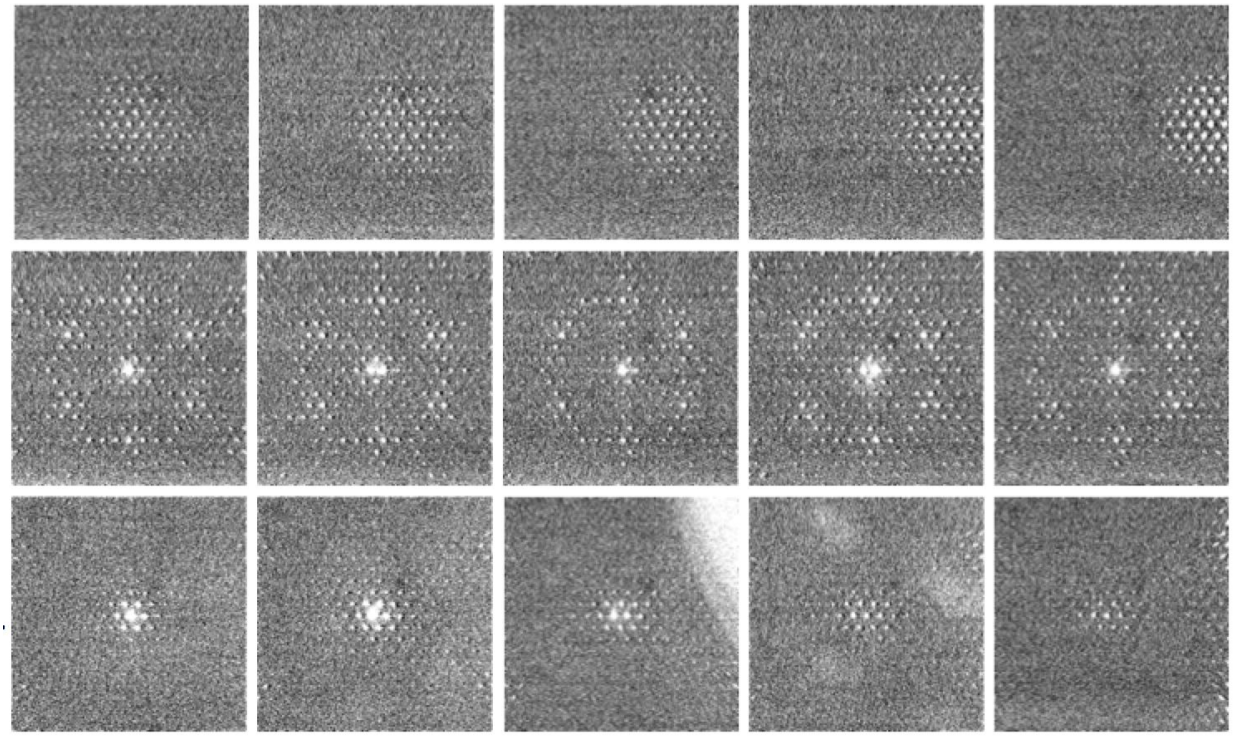

Figure 11. Off-axis focal plan for BIGRE[+1] (top), BIGRE[−1] (middle) and BIGRE[+1−1] (bottom).

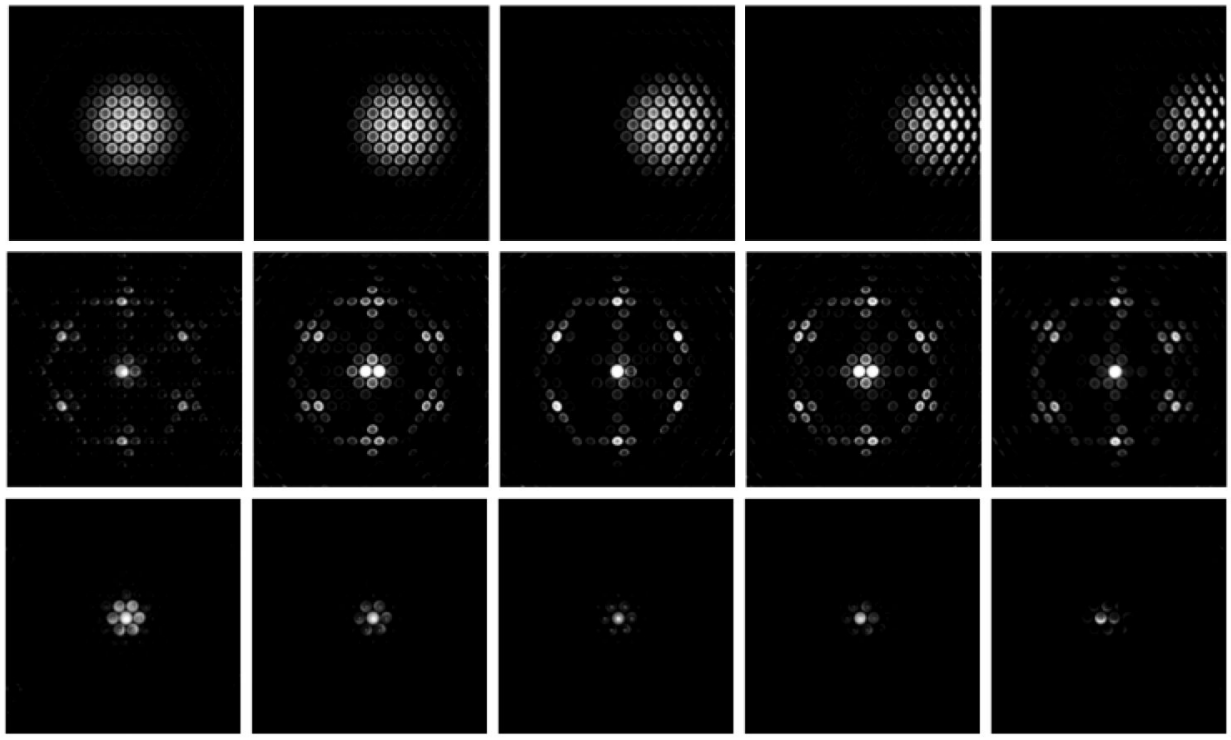

Figure 12. Off-axis extra-focal plan for BIGRE[+1] (top), BIGRE[−1] (middle) and BIGRE[+1−1] (bottom).

5. DISCUSSION

We have examined in this paper not only the light properly propagated and focused in the focal plane, but also the light scattered within the device and diverging - in principle - outside of the CCD camera. For that, a short focal length has been set for the camera lens, enabling to image this parasitic light at the edge of the CCD screen. The next step would be to enlarge the focal length in order to reject this unwished light outside of the CCD camera, to increase the resolution of the image for resolving the Airy pattern, and to zoom onto the useful field of view in the inner part of the image. We should also use a camera with a higher dynamic range to estimate the high contrast imaging capability of such devices.

A forthcoming paper will include more accurate results by means of data processing. A quantitative analysis will be pursued to validate those preliminary results showing the optical behaviour of a BIGRE device. We will also address the tolerance for the alignment of the devices, mainly the sensitivity of BIGRE to the tip-tilt, the position along the optical axis of the BIGRE pupil to be conjugated with the entrance pupil, as well as the differential errors between BIGRE[+1] and BIGRE[−1] for the BIGRE[+1−1] scheme. Finally, to characterize the chromatic effects of such BIGRE devices , we will use a white laser source with narrow-band filters.

6. CONCLUSION

The pupil discretization by means of spatial filtering yields to novel applications for interferometric direct imaging (DAM, DAD) or Fourier imaging (DADI), enabling innovative projects suitable for large telescopes (DAM, DADI) or for long baseline interferometry (DAD). This paper deals with the first in-lab experiment at visible wavelength of BIGRE devices for the three configurations above. We study the point spread function (PSF) when observing a point-like object located either on-axis or at various off-axis positions across the field of view. Both interferometric and diffractive effects are described. The idea to exploit BIGRE in various configurations in a collimated beam has been a success to look at different regimes of light propagation. The experimental measurements are in good agreement with the BIGRE theory. It results that BIGRE fulfils the requirements to carry out spatially filtered pupil discretization (DAM), with possible densification (DAD) or dilution (DADI). In particular, the laboratory results shown in this paper enable to validate the off-axis stability of the Window function and to highlight the spatial filtering properties of the innovative BIGRE-DAM concept.

References

[1] Patru, F., Antichi, J., and Girard, J., "Direct imaging with a dense aperture masking in comparison with a telescope or a hypertelelescope," in [*Society of Photo-Optical Instrumentation Engineers (SPIE) Conference Series*], *Proc. SPIE* **8172**, 0 (Oct. 2011).

[2] Patru, F., Antichi, J., Mawet, D., Jolissaint, L., Carbillet, M., Milli, J., Girard, J., Rabou, P., Giro, E., and Mourard, D., "Discretized aperture mapping with a micro-lenses array for interferometric direct imaging," in [*Society of Photo-Optical Instrumentation Engineers (SPIE) Conference Series*], *Proc. SPIE* **9148**, 5 (Aug. 2014).

[3] Patru, F., Carbillet, M., Jolissaint, L., Mawet, D., and Antichi, J., "Discretized Aperture Mapping for wavefront sensing," in [*This proceeding*], *Proc. SPIE* (2016).

[4] Antichi, J., Dohlen, K., Gratton, R. G., Mesa, D., Claudi, R. U., Giro, E., Boccaletti, A., Mouillet, D., Puget, P., and Beuzit, J.-L., "BIGRE: A Low Cross-Talk Integral Field Unit Tailored for Extrasolar Planets Imaging Spectroscopy," *Astrophysical Journal* **695**, 1042–1057 (2009).

[5] Antichi, J., Rabou, P., Patru, F., Giro, E., Girard, J., and Mourard, D., "The hypertelescope at work with a BIGRE integral field unit," in [*Society of Photo-Optical Instrumentation Engineers (SPIE) Conference Series*], **8172** (2011).

[6] Zeiders, G. W. and Montgomery, E. E., "Diffraction effects with segmented apertures," in [*Space Telescopes and Instruments V*], Bely, P. Y. and Breckinridge, J. B., eds., *Proc. SPIE* **3356**, 799–809 (Aug. 1998).

[7] Yaitskova, N., Dohlen, K., and Dierickx, P., "Analytical study of diffraction effects in extremely large segmented telescopes," *Journal of the Optical Society of America A* **20**, 1563–1575 (2003).

[8] Perrin, G., Lacour, S., Woillez, J., and Thiébaut, É., "High dynamic range imaging by pupil single-mode filtering and remapping," *Monthly Notices of the Royal Astronomical Society* **373**, 747–751 (2006).

[9] Labeyrie, A., "Resolved imaging of extra-solar planets with future 10-100km optical interferometric arrays.," *Astronomy and Astrophysics, Supplement* **118**, 517–524 (1996).

[10] Lardière, O., Martinache, F., and Patru, F., "Direct imaging with highly diluted apertures - I. Field-of-view limitations," *Monthly Notices of the Royal Astronomical Society* **375**, 977–988 (2007).

[11] Patru, F., Tarmoul, N., Mourard, D., and Lardière, O., "Direct imaging with highly diluted apertures - II. Properties of the point spread function of a hypertelescope," *Monthly Notices of the Royal Astronomical Society* **395**, 2363–2372 (2009).

[12] Patru, F., Chiavassa, A., Mourard, D., and Tarmoul, N., "Direct imaging with a hypertelescope of red supergiant stellar surfaces," in [*Society of Photo-Optical Instrumentation Engineers (SPIE) Conference Series*], *Proc. SPIE* **7734**, 42 (2010).

[13] Patru, F., Mourard, D., Clausse, J., Delage, L., Reynaud, F., Dubreuil, M., Bonneau, D., Bosio, S., Bresson, Y., Hugues, Y., Lardière, O., and Roussel, A., "First results from a laboratory hypertelescope using single-mode fibers," *Astronomy and Astrophysics* **477**, 345–352 (2008).

[14] Patru, F., Mourard, D., Lardière, O., and Lagarde, S., "Optimization of the direct imaging properties of an optical-fibred long baseline interferometer," *Monthly Notices of the Royal Astronomical Society* **376**, 1047–1053 (2007).

[15] Mourard, D., Dali Ali, W., Meilland, A., Tarmoul, N., Patru, F., Clausse, J. M., Girard, P., Hénault, F., Marcotto, A., and Mauclert, N., "Group and phase delay sensing for cophasing large optical arrays," *Monthly Notices of the Royal Astronomical Society* **445**, 2082–2092 (2014).

[16] Le Coroller, H., Dejonghe, J., Arpesella, C., Vernet, D., and Labeyrie, A., "Tests with a Carlina-type hypertelescope prototype. I. Demonstration of star tracking and fringe acquisition with a balloon-suspended focal camera," *Astronomy and Astrophysics* **426**, 721–728 (Nov. 2004).

[17] Labeyrie, A., Ballouard, M., Bondoux, E., Bosio, S., Dali-Ali, W., Lacamp, B., Lépine, T., Maillot, J., Mourard, D., Nunez, P. D., Pijoan, J., Prudhomme, R., Riaud, P., Roussel, M., Surya, A., and Tregon, B., "Building a hypertelescope: prototype testing and perspective toward kilometric versions," in [*This proceeding*], *Proc. SPIE* (2016).

[18] Lacour, S., Tuthill, P., Amico, P., Ireland, M., Ehrenreich, D., Huelamo, N., and Lagrange, A.-M., "Sparse aperture masking at the VLT. I. Faint companion detection limits for the two debris disk stars HD 92945 and HD 141569," *Astronomy and Astrophysics* **532**, A72+ (2011).

[19] Martinache, F., "Kernel Phase in Fizeau Interferometry," *Astrophysical Journal* **724**, 464–469 (Nov. 2010).

[20] Wallner, O., Leeb, W. R., and Flatscher, R., "Design of spatial and modal filters for nulling interferometers," in [*Interferometry for Optical Astronomy II*], Traub, W. A., ed., *Proc. SPIE* **4838**, 668–679 (Feb. 2003).

[21] Goodman, J. W., [*Introduction to Fourier optics*], Roberts and Company Publishers (2005).

[22] Gillet, S., Riaud, P., Lardière, O., Dejonghe, J., Schmitt, J., Arnold, L., Boccaletti, A., Horville, D., and Labeyrie, A., "Imaging capabilities of hypertelescopes with a pair of micro-lens arrays," *Astronomy and Astrophysics* **400**, 393–396 (2003).